Am J Physiol Endocrinol Metab 315: E258–E266, 2018.
First published February 6, 2018; doi:10.1152/ajpendo.00386.2017.

RESEARCH ARTICLE | *Translational Physiology*

Acute activation of pyruvate dehydrogenase increases glucose oxidation in muscle without changing glucose uptake

Lewin Small,[1] Amanda E. Brandon,[1,2] Lake-Ee Quek,[3] James R. Krycer,[4] David E. James,[4] Nigel Turner,[5] and Gregory J. Cooney[1,2]

[1]*Diabetes and Metabolism Division, Garvan Institute, Sydney, New South Wales, Australia;* [2]*School of Medical Science, The University of Sydney, Charles Perkins Centre, New South Wales, Australia;* [3]*School of Mathematics and Statistics, The University of Sydney, Charles Perkins Centre, New South Wales, Australia;* [4]*School of Life and Environmental Science, The University of Sydney, Charles Perkins Centre, New South Wales, Australia; and* [5]*Department of Pharmacology, School of Medical Science, University of New South Wales, Sydney, New South Wales, Australia*

Submitted 19 October 2017; accepted in final form 1 February 2018

Small L, Brandon AE, Quek L-E, Krycer JR, James DE, Turner N, Cooney GJ. Acute activation of pyruvate dehydrogenase increases glucose oxidation in muscle without changing glucose uptake. *Am J Physiol Endocrinol Metab* 315: E258–E266, 2018. First published February 6, 2018; doi:10.1152/ajpendo.00386.2017.—Pyruvate dehydrogenase (PDH) activity is a key component of the glucose/fatty acid cycle hypothesis for the regulation of glucose uptake and metabolism. We have investigated whether acute activation of PDH in muscle can alleviate the insulin resistance caused by feeding animals a high-fat diet (HFD). The importance of PDH activity in muscle glucose disposal under insulin-stimulated conditions was determined by infusing the PDH kinase inhibitor dichloroacetate (DCA) into HFD-fed Wistar rats during a hyperinsulinemic-euglycemic clamp. Acute DCA infusion did not alter glucose infusion rate, glucose disappearance, or hepatic glucose production but did decrease plasma lactate levels. DCA substantially increased muscle PDH activity; however, this did not improve insulin-stimulated glucose uptake in insulin-resistant muscle of HFD rats. DCA infusion increased the flux of pyruvate to acetyl-CoA and reduced glucose incorporation into glycogen and alanine in muscle. Similarly, in isolated muscle, DCA treatment increased glucose oxidation and decreased glycogen synthesis without changing glucose uptake. These results suggest that, although PDH activity controls the conversion of pyruvate to acetyl-CoA for oxidation, this has little effect on glucose uptake into muscle under insulin-stimulated conditions.

glucose oxidation; hyperinsulinemic-euglycemic clamp; insulin resistance; muscle insulin action; Randle cycle

INTRODUCTION

Over half a century ago, Randle, Garland, Hales, and Newsholme (36) postulated that glucose and fatty acid uptake and oxidation were controlled by a competitive glucose-fatty acid cycle. This cycle was proposed to be an adaptation to nutrient availability, so that high levels of either plasma glucose or fatty acid could be preferentially utilized. Additionally, this hypothesis was one of the first to attempt to explain the interaction between muscle, the major site of insulin-stimulated glucose disposal in the body, and adipose tissue, the major site for fatty acid release (16).

The cellular mechanisms of the glucose/fatty acid cycle involve the regulation of pyruvate dehydrogenase (PDH), responsible for the production of glucose-derived acetyl-CoA in the mitochondria for use in the tricarboxylic acid (TCA) cycle. PDH is regulated both allosterically via mitochondrial acetyl-CoA concentration as well as posttranscriptionally by both phosphorylation and acetylation (32). Phosphorylation and inactivation of PDH is carried out by PDH kinases (PDKs), of which there are four isoforms with varying tissue distribution in mammals (3). One of these isoforms, PDK4, is upregulated in the muscle of high-fat diet-fed (HFD) rodents (14, 23, 37, 38, 48) and insulin-resistant human subjects (24, 28). Regulation of PDH has therefore been hypothesized to be a possible target in overcoming lipid-induced insulin resistance (25, 41).

To investigate the importance of PDH activity in the regulation of glucose uptake and to test the hypothesis that increased PDH activity can improve insulin sensitivity in muscle, we utilized the PDK inhibitor, dichloroacetate (DCA), a structural analog of pyruvate, which itself inhibits PDKs at high concentrations (20). DCA has been shown to lower fasting blood glucose in both rodents (2, 41) and humans (43), independently of insulin. However, to the best of our knowledge, there are no studies investigating the effect of acute DCA treatment on insulin-stimulated glucose disposal in vivo in the context of an HFD. Therefore, we performed hyperinsulinemic-euglycemic clamps with glucose tracers on chow and HFD rats given an infusion of DCA or an equal volume of saline during the clamp to assess glucose homeostasis and measure insulin sensitivity in vivo. We also acquired tissue-specific glucose uptake and glycogen storage data and examined changes in metabolite abundance. Further studies employing ex vivo muscle incubations to further explore the role of DCA on glucose oxidation confirmed that altering PDH activity changes the balance between glucose and fatty acid oxidation in muscle but has little effect on insulin-stimulated glucose uptake.

MATERIALS AND METHODS

Animals. All surgical and experimental procedures performed were approved by the Garvan Institute/St. Vincent's Hospital Animal Eth-

Address for reprint requests and other correspondence: G. Cooney, Univ. of Sydney, Charles Perkins Centre, D17, Sydney Medical School Sydney, NSW, 2006 (e-mail: gregory.cooney@sydney.edu.au).

ics Committee and were in accordance with the National Health and Medical Research Council of Australia's guidelines on animal experimentation. Adult male Wistar rats (Animal Resources Centre, Perth, Australia) were communally housed in temperature-controlled (22 ± 0.5°C) 12-h:12-h light-dark cycle rooms. Rats (100–120 g) were fed ad libitum a standard chow diet (Rat Maintenance Diet; Gordon Specialty Feeds, Sydney, Australia) or a lard-based high-fat, high-sucrose diet [calorically, 48% fat, 34% carbohydrate (17% starch, 17% sucrose), 18% protein] (HFD) made in house, for 4 wk. After 3 wk of a diet, chronic cannulae were inserted into the right jugular vein and left carotid artery. Rats recovered for 1 wk before the clamp procedure.

Hyperinsulinemic-euglycemic clamp. Details of the clamp procedure have been reported previously (30, 47). Animals (5 h fasted) were studied over 2.5 h in the conscious state, and HFD animals were randomly divided into groups to receive saline or DCA infusion. DCA (Sigma-Aldrich, Castle Hill, Australia) was neutralized with NaOH, filter sterilized, and made up for each animal so that they received 100 $mg \cdot kg^{-1} \cdot h^{-1}$ in a volume of 2 ml/h. A basal blood sample was taken, and the animals received a bolus of either DCA (100 mg/kg) or an equal volume of saline; then, an infusion of either saline or DCA (100 $mg \cdot kg^{-1} \cdot h^{-1}$) was started, which continued over the entire course of the clamp procedure (Fig. 1). Blood samples were taken to determine the effect of DCA on blood analytes in the basal period. After 30 min of saline or DCA infusion, a constant infusion of insulin (Actrapid; Novo Nordisk, Copenhagen, Denmark) was started ($0.3\ U \cdot kg^{-1} \cdot h^{-1}$) and a variable rate of glucose were infused (30% wt/vol) to maintain plasma glycemia between 7 and 8 mM. Once plasma glucose levels reached steady state, a bolus of [^{14}C (U)]glucose, 2-deoxy[^{3}H 1,2 (N)]glucose (PerkinElmer, Glen Waverly, Australia) tracer was administered, and blood samples were taken over the next 45 min to provide plasma disappearance curves for radioactive tracers. At the conclusion of the clamp, animals were administered a lethal dose of pentobarbital (intravenously), and tissues were rapidly dissected (starting with heart and muscles) and freeze clamped for determination of glucose uptake, metabolite concentrations, and enzyme assays. The glucose infusion rate (GIR) was measured as the volume of glucose infused into the animal during steady state (Fig. 1*A*).

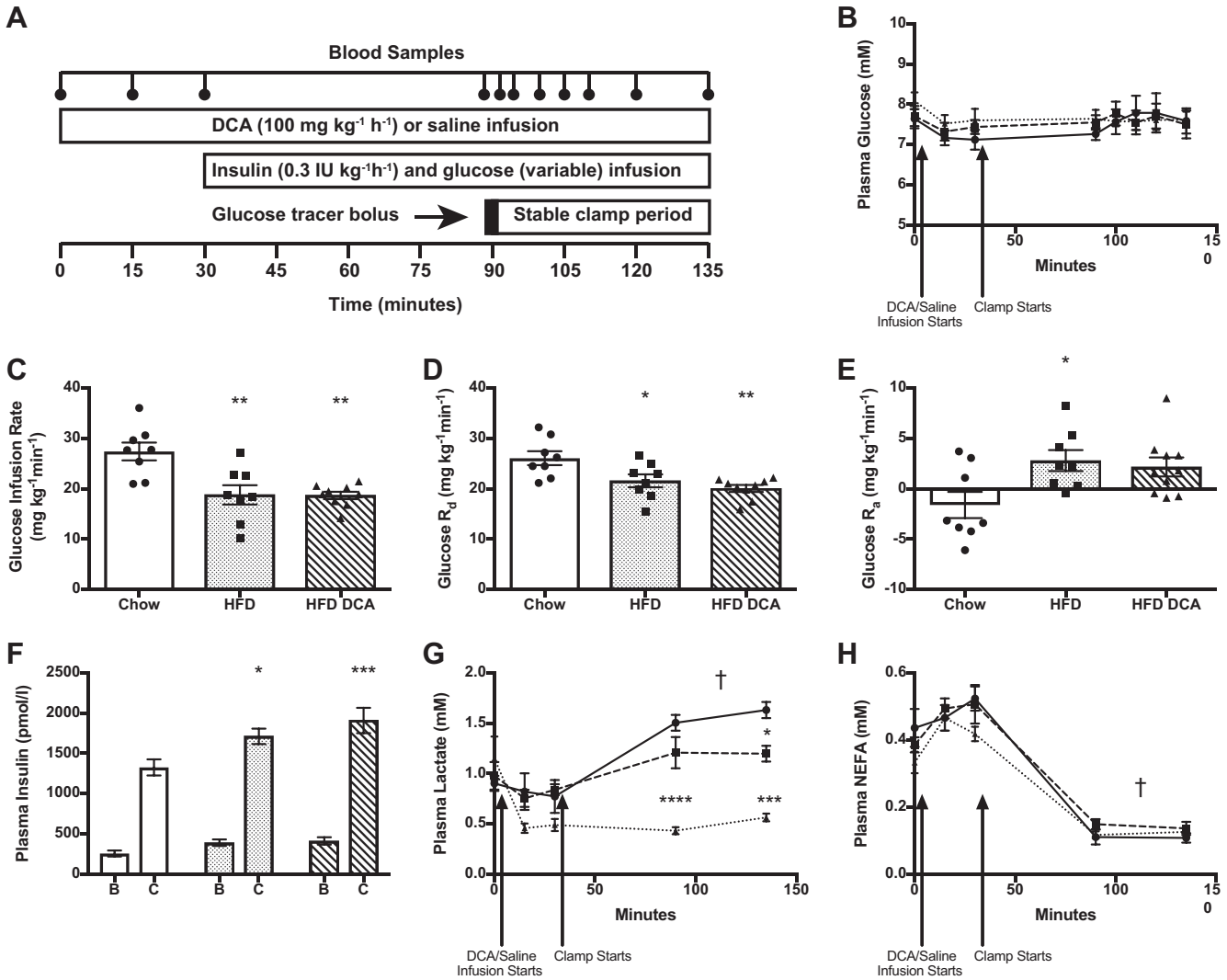

Fig. 1. Systemic substrate handling during hyperinsulinemic-euglycemic clamp. Chow is shown by the open bar and solid line, high fat diet (HFD) is the dotted bar and dashed line, and HFD dichloroacetate (DCA) is the hatched bar and dotted line. *A*: schematic of hyperinsulinemic-euglycemic clamp. *B*: plasma glucose over clamp period. *C*: glucose infusion rate during stable clamp period. *D*: rate of glucose disappearance (R_d) during stable clamp period. *E*: rate of glucose appearance (R_a) during stable clamp period. *F*: basal (B) and clamped (C) plasma insulin. *G*: plasma lactate over clamp period. *H*: plasma nonesterified fatty acid (NEFA) over clamp period, $n = 8$. Analyzed by 1-way ANOVA or repeated-measures, 2-way ANOVA for an effect of group and an effect of clamp. *$P < 0.05$, **$P < 0.005$, ***$P < 0.0005$, ****$P < 0.0001$ compared with chow. †$P < 0.005$ main effect of clamp.

Blood/plasma analysis. Blood glucose during the clamp was determined via glucometer (Accu-Chek Perfoma; Roche Diagnostics, Castle Hill, Australia), and plasma glucose was determined by glucose oxidase assay (Infinity GOx; Thermo Fisher, Scoresby, Australia). Plasma insulin was determined by ELISA (mouse ultrasensitive; Crystal Chem, Elk Grove Village, IL), and nonesterified fatty acid (NEFA) in the plasma was determined by NEFA kit (Wako Diagnostics, Mountain View, CA). Lactate in plasma was determined after protein precipitation with 6% perchloric acid (PCA) and neutralizing using 1 M NaOH by measuring production of NADH from NAD^+ by lactate dehydrogenase in the presence of 0.4 M hydrazine hydrate as previously described (10).

Tracer analytical methods. Plasma and tissue levels of ^{3}H- and ^{14}C-labeled glucose tracers were measured to calculate whole body glucose disposal rate (R_d), to estimate tissue glucose uptake (R_g'), and to measure incorporation of glucose into glycogen. Assays and calculations for the glucose disappearance, glucose uptake into tissues, and glucose incorporation into glycogen and glycogen content measures were as previously described (19, 31).

Enzyme assays. PDH assay was performed on crude extracts of frozen tissue with the addition of kinase and phosphatase inhibitors (1 mM DCA, 10 mM NaF) by coupling with arylamine acetyltransferase and following the change in absorbance of 4-aminoazobenzene-4'-sulfonic acid (AABS) at 390 nm as it becomes acetylated as described by Coore et al. (9). The assay was conducted in 100 mM Tris containing 1.0 mM $MgCl_2$, 1.0 mM EDTA, 0.2 mM CoA, 1.0 mM NAD^+, 1.0 mM thiamine pyrophosphate, 20.0 μg/ml AABS, and excess arylamine acetyltransferase (extracted from pigeon liver acetone powder; Sigma-Aldrich), pH 7.8 and initiated with the addition of sodium pyruvate to a final concentration of 2.0 mM. Citrate synthase activity was determined as previously described (45).

Immunoblotting. Frozen, powdered tissue was homogenized by probe homogenizer in RIPA buffer containing protease inhibitor cocktail (EDTA free; Roche) and phosphatase inhibitors (NaF, Na_3VO_4). Tissue lysates were subjected to SDS-PAGE, transferred to PVDF membranes, blocked in 2% BSA, and then immunoblotted with antibodies for pPDH E1α (S293) (Millipore, Macquarie Park, Australia), PDH E1α total H-131 (Santa Cruz Biotechnology, Santa Cruz, CA), pAkt (S473), and pan Akt (Cell Signaling Technology, Beverly, MA). Densitometry analysis was performed using ImageJ software (NIH; https://imagej.nih.gov/ij/).

Metabolite extraction and liquid chromatography-mass spectrometry. Amino acids and central carbon metabolite concentrations were measured based on the positive/negative ion-switching liquid chromatography-mass spectrometry (LC-MS) method described by Yuan et al. (49). Briefly, 25 mg of powdered muscle tissue was homogenized in 500 μl 50% (vol/vol) methanol:water mixture containing internal standards 2-morpholinoethanesulfonic acid and D-camphor-10-sulfonic acid at 2.5 μM. A sample (500 μl) of chloroform was added to the extracts and vortexed. The aqueous phase was separated from the insoluble and organic layers by centrifugation and was stored at −30°C. LC-MS analysis was performed using an Agilent Infinity 1260 LC coupled to an AB Sciex QTRAP 5500 MS. LC separation was achieved on a XBridge Amide column (2.1-mm inner diameter, 100-mm length; Waters, Dundas, Australia) at ambient temperature using buffer A [95:5 (vol/vol) water:acetonitrile containing ammonium hydroxide and ammonium acetate both at 20 mM (pH 9.3)] and buffer B (100% acetonitrile). A sample (2.5 μl) of the supernatant was injected, and metabolites were eluted using flow rate and gradients described by Yuan et al. (49). MS ion source temperature was set at 350°C. Multiple reaction-monitoring acquisition was performed with a 40-ms dwell time. Calibration standards were injected using the same set up. Raw data were extracted into text files using ProteoWizard. Peak alignment and integration were performed using in-house MATLAB (The MathWorks) scripts.

Ex vivo glucose uptake, glucose oxidation, glycogen synthesis, and oleate oxidation. Soleus muscles from a separate cohort of HFD rats were dissected tendon to tendon into strips (~30 mg) and incubated in warmed (30°C), pregassed (95% O_2-5% CO_2, pH 7.4), modified Krebs-Henseleit buffer (KHB) containing 5 mM glucose, 10 mM HEPES, and 1% BSA. Following a 30-min preincubation period ± 1 mM DCA, muscle strips were transferred to a new vial containing 1.5 ml of the above medium plus 37.0 kBq/ml 2-deoxy[^{3}H] glucose and 37.0 kBq/ml [^{14}C]glucose ± insulin (1.0 mU/ml) ± 1.0 mM DCA for 60 min, containing an open microfuge tube of 200.0 μl of 1.0 M NaOH. At the conclusion of the incubation period, muscle strips were blotted dry and snap frozen. Media in the scintillation vials was acidified with the addition of 200 μl of 25% PCA, and the lid was quickly screwed back on. The vials were left for 2 h for the capture of released $^{14}CO_2$ by the NaOH solution, which was determined by liquid scintillation counting. Muscle strips were halved and weighed for glucose uptake and glucose incorporation into glycogen as previously described (19, 31). Oleate oxidation was carried out identically to glucose oxidation, in the same modified KHB buffer but with the inclusion of 2.0% BSA, 0.5 mM oleic acid (conjugated to the BSA at 37°C for 1 h), and 37.0 kBq/ml [1-^{14}C] oleic acid (without glucose tracers), in separate soleus strips. ^{14}C-labeled acid-soluble metabolites resulting from oleate oxidation were determined by liquid scintillation counting of the acidified media.

Statistical analysis. Data are presented as means ± SE. Statistical significance was determined by one- or two-way ANOVA as appropriate using GraphPad Prism (Version 7; San Diego, CA). When ANOVA reached significance, Tukey's post hoc test was conducted to test comparisons. Metabolomics data were corrected for multiple comparisons by the Holm-Sidak test. Significance was set at $P < 0.05$.

RESULTS

Acute DCA treatment does not affect systemic glucose disposal under insulin-stimulated conditions. Animals in the HFD control and DCA-treated groups were matched for body weight, and there was no significant difference between the body or fat pad weights of saline- and DCA-treated HFD rats. HFD animals had significantly increased fat pad weights compared with chow controls (Table 1). To assess the effects of acutely activating PDH in vivo, we performed hyperinsulinemic-euglycemic clamps on Wistar rats infused with either saline or 100 $mg \cdot kg^{-1} \cdot h^{-1}$ of DCA (Fig. 1*A*). Because of its short half-life (42), DCA-administered animals were given a priming bolus (100 mg/kg) followed by an infusion of DCA (100 $mg \cdot kg^{-1} \cdot h^{-1}$). This dose is at the high end of those that have been used clinically; however, similar doses have been reported to be well tolerated in humans (11) and shown to

Table 1. *Body and fat pad weights and metabolic characteristics of clamped rats*

Group	Chow Saline	HFD Saline	HFD DCA
Body weight, g	320.6 ± 4.6	337.1 ± 7.3	340.1 ± 11.3
Epididymal fat pad weight, g	2.2 ± 0.2	3.6 ± 0.4*	4.1 ± 0.4‡
Inguinal fat pad weight, g	3.7 ± 0.3	5.6 ± 0.6*	6.1 ± 0.6†
Retroperitoneal fat pad weight, g	2.9 ± 0.2	5.1 ± 0.4†	5.1 ± 0.4‡
Clamped plasma glucose, mM	7.3 ± 0.3	7.3 ± 0.3	7.3 ± 0.2
Basal NEFA, mM	0.45 ± 0.04	0.41 ± 0.02	0.37 ± 0.03
Clamped NEFA, mM	0.11 ± 0.02	0.14 ± 0.02	0.11 ± 0.01
NEFA suppression, %	73.9 ± 4.0	63.3 ± 4.8	67.3 ± 3.9

Values are means ± SE, $n = 8$, analyzed by 1-way ANOVA. HFD, high-fat diet; DCA, dichloroacetate; NEFA, nonesterified fatty acid. *$P < 0.05$, †$P < 0.005$, ‡$P < 0.0005$ compared with chow controls.

provide good bioavailability after oral administration in rats (39). Basal glucose levels did not change significantly over 30 min of DCA infusion compared with saline-infused animals (Fig. 1*B*). During the clamp, plasma glucose was successfully clamped between 7 and 8 mM (Fig. 1*B*). HFD animals had a decreased glucose infusion rate during the hyperinsulinemic-euglycemic clamp (~70% of chow); however, there was no difference between DCA-and saline-treated animals (Fig. 1*C*). The rate of whole body glucose disappearance showed a similar pattern with a decrease with fat feeding (~80% of chow); however, DCA treatment had no effect (Fig. 1*D*). Hepatic glucose output was completely suppressed in chow animals and was not different between DCA- and saline-treated HFD rats (Fig. 1*E*). Plasma insulin levels during the clamp were comparable between HFD groups but were slightly lower in chow animals, possibly reflecting lower basal insulin levels in the chow animals. Basal insulin levels were not different between saline- and DCA-treated HFD groups (Fig. 1*F*). Plasma lactate levels were increased by the clamp procedure compared with basal levels in the chow and HFD groups (Fig. 1*G*). The chow animals had significantly higher plasma lactate compared with HFD animals at the end of the clamp, reflecting the higher glucose disposal. DCA treatment completely suppressed the increase in plasma lactate produced by the hyperinsulinemic-euglycemic clamp without altering glucose disposal, suggesting a possible reduction in nonoxidative glucose utilization. Plasma NEFA levels were suppressed by the clamp with no differences between groups (Fig. 1*H*).

Acute DCA treatment activates muscle PDH without changing glucose uptake. DCA treatment significantly and substantially increased PDH activity in the red quadriceps (RQ) and tibialis cranialis (TC) muscles (~8-fold) and heart (~2-fold) (Fig. 2*A*). HFD muscle had significantly reduced PDH activity compared with chow; however, this was not seen in the heart. Additionally, phosphorylation of PDH E1α at the serine 293 residue was markedly reduced after DCA treatment in both RQ and TC muscle; however, there was no effect of diet (Fig. 2, *B* and *C*). This suggests that the dose of DCA was sufficient to

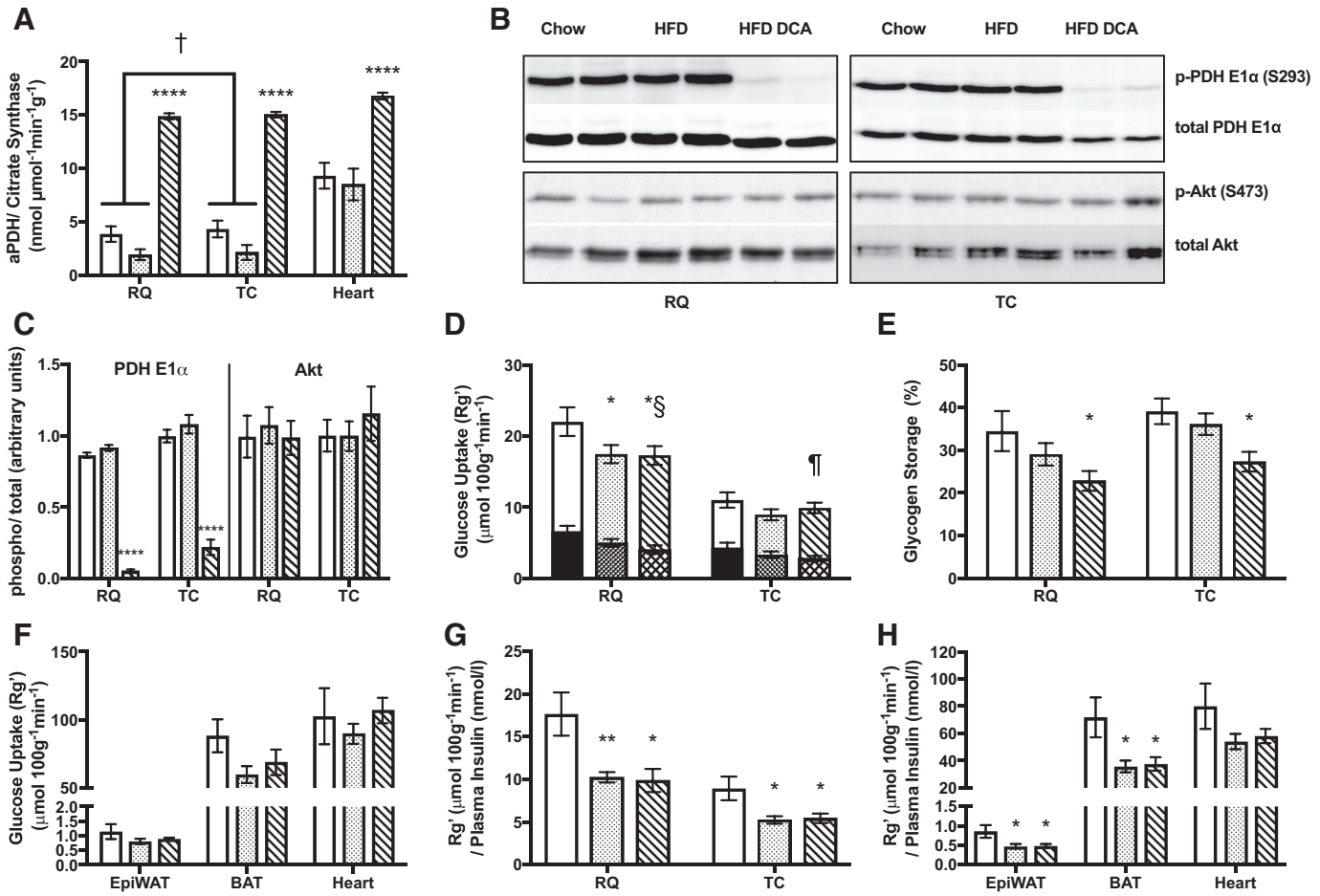

Fig. 2. Dichloroacetate (DCA) increases pyruvate dehydrogenase (PDH) activity in muscle without changing glucose uptake. Chow is the open bar, high-fat diet (HFD) is the dotted bar, and HFD DCA is the hatched bar. *A*: active PDH activity normalized to citrate synthase activity in red quadriceps (RQ) and tibialis cranialis (TC) muscles and heart. *B*: representative immunoblot of phospho (S293) and total PDH E1α and phospho (S473) and total Akt in RQ and TC muscle. *C*: densitometry of PDH and Akt phosphorylation (phospho/total). *D*: rate of glucose uptake (total bar) and the proportion of this rate incorporated into glycogen (bottom bar) in RQ and TC muscles. *E*: percent of glucose uptake incorporated into glycogen in RQ and TC muscles. *F*: rate of glucose uptake into epididymal white adipose tissue (epiWAT), brown adipose tissue (BAT), and heart. Rate of glucose uptake normalized to clamp plasma insulin in muscle (*G*), epiWAT, BAT, and heart (*H*) (R_g'/plasma insulin); $n = 8$, analyzed by 1-way ANOVA. $^*P < 0.05$, $^{**}P < 0.005$, $^{****}P < 0.0001$ compared with chow. †$P < 0.05$ for an effect of diet over both muscles (2-way ANOVA). §$P < 0.05$ for glucose incorporation into glycogen compared with chow. ¶$P = 0.06$ for glucose incorporation into glycogen compared with chow.

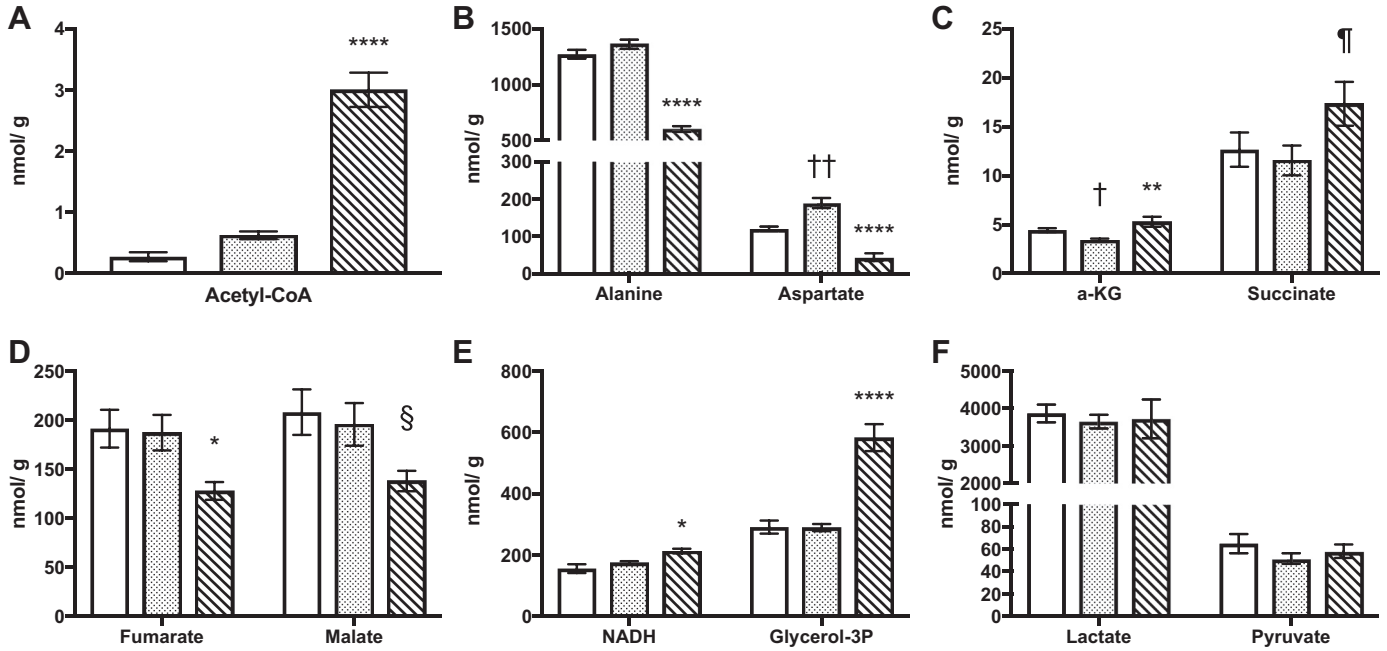

Fig. 3. Dichloroacetate (DCA) alters metabolic equilibrium in red quadriceps muscle around the pyruvate node. Values are nanomoles/gram (wet weight). Chow is the open bar, high-fat diet (HFD) is the dotted bar, and HFD DCA is the hatched bar. *A*: acetyl-CoA. *B*: alanine and aspartate. Early (*C*) and late (*D*) tricarboxylic acid cycle intermediates and α-ketoglutarate (a-KG) are shown. *E*: NADH and glycerol-3-phosphate. *F*: lactate and pyruvate, $n = 8$, analyzed by 1-way ANOVA. $^{*}P < 0.05$, $^{**}P < 0.005$, $^{****}P < 0.0001$, §$P = 0.14$, ¶$P = 0.09$ compared with HFD control. †$P < 0.05$, ††$P < 0.0005$ compared with chow control.

substantially increase PDH activity in vivo. Akt phosphorylation at the serine 473 residue measured in both the RQ and TC muscle at the end of the clamp was not altered by either diet or DCA treatment (Fig. 2, *B* and *C*). Fat feeding significantly reduced the rate of glucose uptake into the RQ (77% of chow control), and this was not altered with DCA treatment (Fig. 2*D*). The rate of glucose incorporation into glycogen was significantly reduced in the RQ of DCA-treated HFD animals compared with chow controls. The whiter TC muscle did not show a significant effect of diet or DCA on glucose uptake; however, TC from DCA-treated animals tended to have a lower rate of glucose incorporation into glycogen than chow controls ($P = 0.06$) (Fig. 2*D*), and the percentage of the rate of glucose uptake that was stored as glycogen was significantly reduced in both the RQ and TC of DCA-treated animals compared with chow-fed controls (Fig. 2*E*). The rate of glucose uptake was not significantly different in the epididymal white adipose tissue, brown adipose tissue (BAT), or heart of HFD animals (Fig. 2*F*). However, if glucose uptake was corrected for the circulating insulin level during the clamp (which was slightly higher in HFD animals compared with chow) (Fig. 1*F*), then glucose uptake was significantly lower in all tissues studied except the heart (Fig. 2, *G* and *H*). Overall, this suggests that, in DCA-treated muscle, glucose is being directed toward oxidation at the expense of glycogen synthesis and without altering total glucose input.

DCA treatment channels pyruvate into acetyl-CoA at the expense of other pathways. To determine the effect of DCA treatment on the concentrations of glucose catabolites in vivo, targeted metabolomics was undertaken on the RQ muscle from clamped animals. DCA treatment significantly and substantially increased muscle acetyl-CoA by approximately fivefold (Fig. 3*A*), indicating increased flux through PDH, similar to reports in human muscle (15). Alanine and aspartate levels in DCA-treated muscle were half that of HFD controls (Fig. 3*B*), suggesting preferential decarboxylation of pyruvate by PDH at the expense of other pathways. This could also be seen in the abundance of TCA cycle intermediates; α-ketoglutarate and succinate were elevated with DCA administration (Fig. 3*C*), whereas fumarate and malate were lowered (Fig. 3*D*). DCA administration increased muscle NADH levels (Fig. 3*E*), presumably as a result of increased PDH activity; however, ATP levels were unchanged (Table 2). Glycerol-3-phosphate levels were also increased, perhaps attributable to increased glycerol-3-phosphate dehydrogenase activity in response to an elevated $NADH/NAD^+$ ratio (Fig. 3*E*). Interestingly, DCA treatment did not significantly change the concentration of either pyruvate or lactate (Fig. 3*F*) or the abundance of glycolytic intermediates apart from phosphoenolpyruvate, which was significantly decreased in the muscle of DCA-treated animals (Table 2).

To further investigate the effect of DCA treatment on glucose uptake and oxidation, we examined the effect of insulin and DCA in isolated muscle strips ex vivo. Insulin stimulated glucose uptake and glycogen synthesis in soleus strips by approximately twofold but had a minimal effect on glucose oxidation (20% increase) (Fig. 4). Adding 1 mM DCA was sufficient to double the rate of glucose oxidation under both insulin-stimulated and basal conditions in HFD soleus muscle (Fig. 4*A*) without any change in glucose uptake (Fig. 4*B*) but a significant effect to reduce glucose conversion to glycogen (Fig. 4*C*). These results are similar to those obtained in vivo, wherein DCA treatment did not significantly affect the rate of glucose uptake but signifi-

Table 2. *Abundance of metabolites in red quadriceps from clamped animals*

Group	Chow Saline	HFD Saline	HFD DCA
Threonine	154 ± 07	259 ± 22*	284 ± 18
Glutamine	1991 ± 95	2167 ± 88	2526 ± 54†
Glutamate	1074 ± 33	1050 ± 38	1106 ± 53
Citrate	93.7 ± 10.1	85.2 ± 7.1	86.6 ± 5.9
NAD^+	264 ± 15	248 ± 12	251 ± 14
ATP	4977 ± 244	4603 ± 193	4718 ± 146
G6P/F6P	1557 ± 227	1342 ± 64	1497 ± 136
F1,6BP	124 ± 34	141 ± 24	159 ± 22
DHAP/GAP	761 ± 113	722 ± 84	797 ± 50
3PG/2PG	52.5 ± 6.6	54.8 ± 5.5	61.1 ± 3.9
PEP	10.5 ± 1.2	9.0 ± 0.8	6.5 ± 0.3†

Values are nanomoles/gram (wet weight), means ± SE, $n = 8$, analyzed by individual 1-way ANOVAs adjusted for multiple comparisons using the Holm-Sidak test. Peaks of some metabolites could not be differentiated between one another and are denoted with a slash between them. HFD, high-fat diet; DCA, dichloroacetate; G6P, glucose-6-phosphate; F6P, fructose-6-phosphate; F1,6BP, fructose-1,6-bisphosphate; DHAP, dihydroxyacetone-phosphate; GAP, glyceradelhyde-3-phosphate; 3PG, 3-phosphogycerate; 2PG, 2-phosphoglycerate; PEP, phosphoenolpyruvate. *$P < 0.05$ compared with chow control. †$P < 0.05$ compared with HFD control.

cantly decreased insulin-stimulated glucose incorporation into glycogen by ~30%. Oleate oxidation was significantly decreased by DCA treatment but was not affected by insulin (Fig. 4*D*). Overall this indicates that increasing glucose oxidation in muscle does not necessarily result in a corresponding increase in glucose uptake.

DISCUSSION

The glucose/fatty acid cycle hypothesis for the regulation of glucose and fatty acid oxidation in tissues was described over half a century ago (36), but there is still significant debate about the role this cycle plays in the modulation of insulin-stimulated glucose uptake in skeletal muscle in normal and insulin-resistant states (8, 13, 33, 35). Skeletal muscle makes a relatively large contribution to postprandial glucose disposal (5) and is therefore an attractive target for novel insulin sensitizers to combat the increasing problem of obesity-related insulin resistance. At the center of the glucose/fatty acid cycle is the regulation of the activity of PDH. Much of the recent work investigating PDH regulation has utilized various forms of PDK knockout animals, which have had varying effects on insulin sensitivity from beneficial (17, 21, 44) to adverse (35). If the glucose/fatty acid cycle is important in substrate regulation, long-term activation of PDH could lead to a reciprocal reduction in fatty acid oxidation, potentially increasing stored lipid. Therefore, genetic models such as the PDK knockout mice might introduce confounding factors, such as increased muscle lipid or other possible transcriptional changes resulting from long-term modulation of substrate oxidation. We believed that acute activation of PDH by DCA infusion provides a

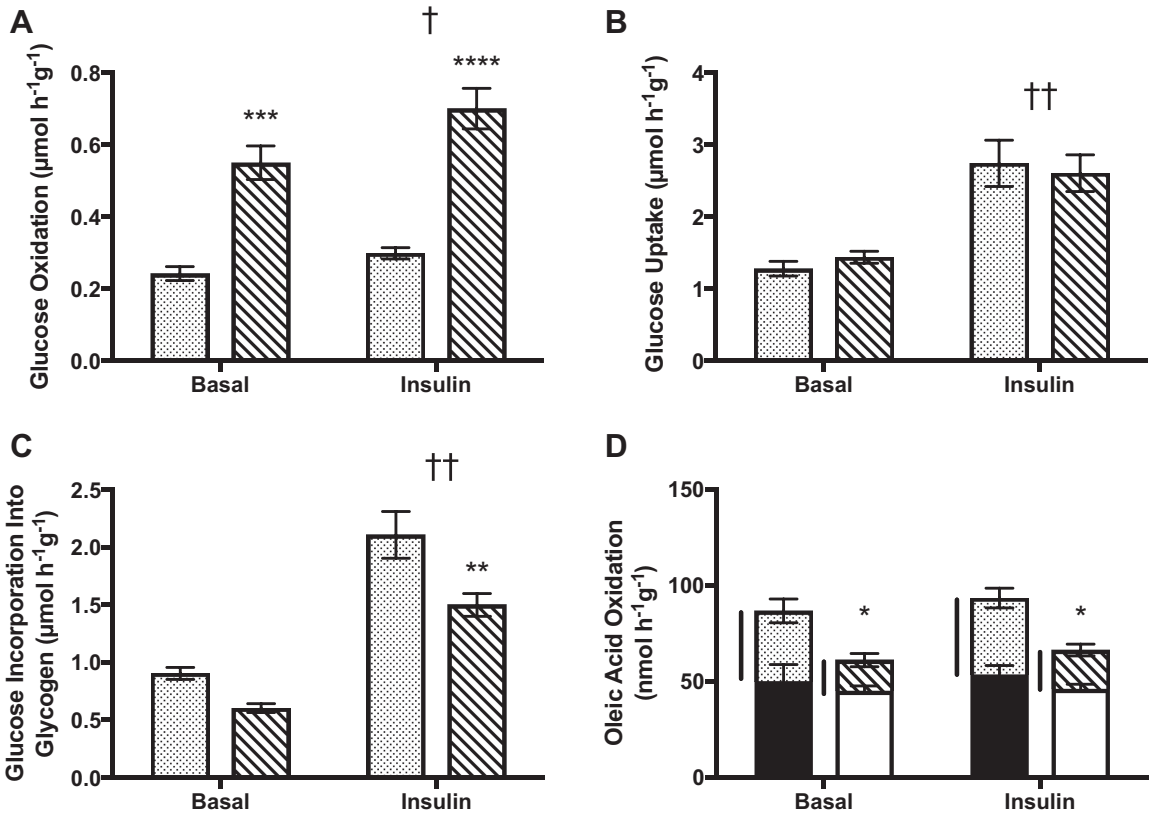

Fig. 4. Dichloroacetate (DCA) increases glucose oxidation and decreases fatty acid oxidation without changing glucose uptake in isolated soleus. Control muscles are dotted bars, and DCA-treated muscles are hatched bars. *A*: rate of glucose oxidation. *B*: rate of glucose uptake. *C*: rate of glucose incorporation into glycogen, $n = 6$. *D*: rate of oleic acid oxidation; bottom bars are acid-soluble metabolites, top bars are $^{14}CO_2$ production, analyzed by 2-way ANOVA. *$P < 0.05$, **$P < 0.005$, ***$P < 0.0005$, ****$P < 0.0001$ compared with control muscles. †$P < 0.05$, ††$P < 0.0001$, main effect of insulin.

good model to investigate the glucose/fatty acid cycle in vivo without introducing these confounding factors.

DCA has been investigated over the last half century for multiple diseases of metabolism, such as PDH deficiency and lactic acidosis, and there is significant literature on its pharmacology and pharmacodynamics. DCA has been shown to consistently lower fasting blood glucose in rodents (2) and humans (4, 43) and may have additive effects with insulin on systemic substrate utilization (1). However, to the best of our knowledge, our study is the first to look at the effects of acutely activating PDH on insulin-stimulated glucose disposal in vivo. Infusion of DCA was sufficient to substantially activate muscle PDH demonstrated by both the loss of phosphorylation at the Serine 293 residue of the E1α subunit and by enzymatic activity (Fig. 2, *A–C*). This was accompanied by an increased amount of acetyl-CoA (Fig. 3*A*), which is indicative of an increased conversion of pyruvate to acetyl CoA by active PDH. Interestingly, this increased activity of PDH had no effect on systemic glucose disposal during a hyperinsulinemic-euglycemic clamp (Fig. 1*C*) or insulin-stimulated glucose uptake in muscle during the clamp (Fig. 2, *D* and *G*). Akt phosphorylation at the serine 473 residue, which is often used as an indication of insulin signaling, was unchanged by DCA administration (Fig. 2, *B* and *C*). Similarly, there was no difference in Akt phosphorylation in the muscle of HFD animals compared with chow controls at the end of the clamp, which has previously been reported by our group (46).

In isolated soleus muscle, DCA treatment did not affect muscle glucose uptake (Fig. 4*B*) despite substantially increasing glucose oxidation (Fig. 4*A*), consistent with previous studies in isolated muscle (6). In ex vivo muscle experiments under basal conditions (Fig. 4), glucose oxidation accounted for ~25% of glucose taken up, which increased to ~45% with DCA treatment. However, under insulin-stimulated conditions, the contribution of glucose oxidation to glucose utilization was reduced to ~17%, and the doubling of glucose oxidation by DCA administration only increased the percentage of glucose taken up that is oxidized to ~30%. This suggests that complete oxidation accounts for less than half of insulin-stimulated glucose disposal in muscle and may explain the reported lower fasting blood glucose levels after DCA treatment because of the higher relative contribution of glucose oxidation to glucose disposal under basal conditions. Interestingly, the reduction in glucose incorporation into glycogen seen in DCA-treated muscle is quantitatively similar to the increase in glucose oxidation, suggesting that the increase in glucose oxidation is supported by changes in intramyocellular glucose partitioning rather than marked changes in glucose uptake into the muscle. A decreased rate of glucose incorporation into glycogen was also observed in the muscle of the DCA-treated rats in vivo (Fig. 2, *D* and *E*). This, together with the substantially decreased plasma lactate as a result of DCA infusion (Fig. 1*G*), suggests that activating PDH increases the oxidation of glucose (Fig. 4*A*), at the expense of fatty acids (Fig. 4*D*), and, to support this, the tissue diverts glucose metabolism away from glycogen storage and lactate production into oxidation without any alteration in glucose uptake. Interestingly, DCA only affected $^{14}CO_2$ production from oleate and not the production of ^{14}C-labeled acid-soluble metabolites resulting from incomplete fatty acid oxidation (Fig. 4*D*). This may suggest that entry of fatty acids into the mitochondria and beta oxidation were not affected by DCA. Instead, because of the large increase in acetyl-CoA abundance after DCA administration (Fig. 3*A*), fatty acid-derived acetyl-CoA must compete with glucose-derived acetyl-CoA for oxidation.

DCA administration did not change muscle lactate concentration (Fig. 3*F*), which is consistent with previous literature in resting human muscle that reported no effect of DCA on lactate and pyruvate concentrations (15). This may be due to increased lactate utilization/uptake with DCA treatment, which has been reported at a systemic level during a lactate clamp after DCA administration (12). The increase in plasma lactate during the clamp (which was greater in the chow animals) indicates that much of the increase in glucose uptake under insulin-stimulated conditions is metabolized via nonoxidative pathways, and a loss of insulin sensitivity may result from a defect in nonoxidative

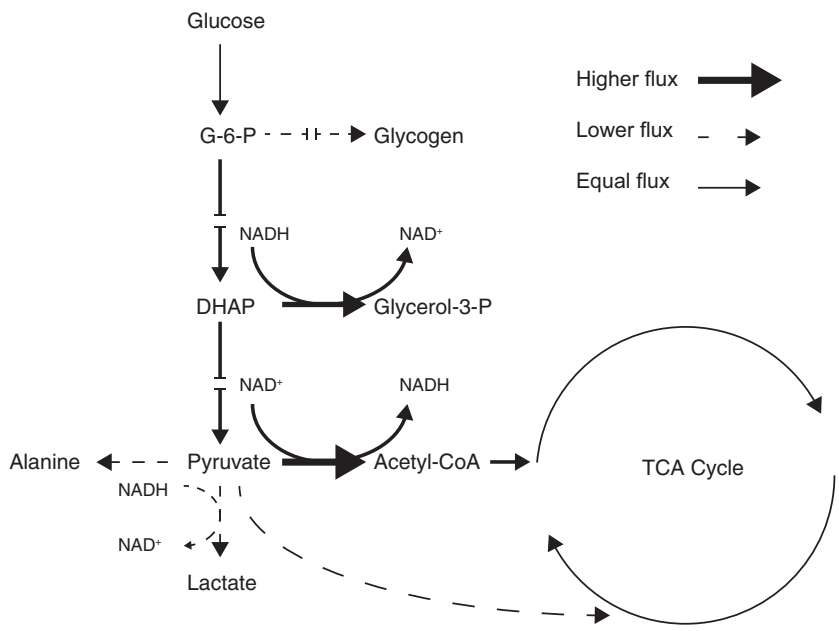

Fig. 5. Schematic of our interpretation of the effect of dichloroacetate in muscle using the above metabolomics and tracer data. Thicker arrows represent an increase in flux compared with control. Dashed arrows represent a decrease in flux compared with control. G-6-P, glucose-6-phosphate; DHAP, dihydroxyacetone-phosphate; TCA, tricarboxylic acid.

glucose metabolism. This idea is supported by both the reduction in insulin-stimulated glycogen synthesis, which is relatively well established (40), as well as reduced lactate appearance that has also been reported in insulin-resistant individuals in response to a glucose load (18, 26, 27, 34).

Both the in vivo glucose tracer and metabolomics data indicate that the main effect of DCA treatment in muscle is to alter the balance of substrate metabolism. DCA treatment increased the abundance of acetyl-CoA (Fig. 3*A*) while decreasing alanine and aspartate (Fig. 3*B*). The reduction in muscle aspartate may reflect diminished malate/oxaloacetate abundance (malate/aspartate shuttle) (Fig. 3*B*). Lower abundance of the TCA cycle intermediates around oxaloacetate after DCA treatment (Fig. 3*C*) may reflect a reduction in flux through pyruvate carboxylase. A simplified schematic of our interpretation of these findings is shown in Fig. 5, where the increased conversion of pyruvate to acetyl-CoA results in a compensatory decrease in glucose metabolism by other pathways.

In resting muscle, the oxidative metabolism of glucose will be linked via oxidative phosphorylation to synthesis of ATP to support the energy requirements of the tissue. The amount of glucose oxidation required to fuel ATP production may therefore only be a small fraction of the total glucose uptake into the muscle, particularly under insulin-stimulated conditions. Without a change in energy demand (e.g., exercise), the increased glucose uptake that occurs in muscle after insulin stimulation is likely to be far greater than required for oxidative metabolism, and therefore therapies aimed at increasing glucose oxidation may not result in meaningful increases in insulin-stimulated glucose uptake. It is possible that tissues with a greater energetic demand such as the heart or activated BAT may benefit from pharmacologically activating PDH, as they are significantly more oxidative than resting muscle. Potentially, in conjunction with exercise (muscle contraction), which can be a more potent stimuli for muscle glucose uptake than insulin alone (29), PDH activation may alter glucose homeostasis (7). On the other side of the glucose/fatty acid cycle, pharmacological inhibition of fatty acid oxidation has been employed with some success to increase glucose uptake into muscle (22, 31). However, this study suggests that these effects are not driven by activation of PDH but by limiting of the major source of energy substrate for muscle in the resting state, fatty acids.

In conclusion, we have shown that acutely activating PDH can increase muscle glucose oxidation and alter nonoxidative glucose metabolism. However, this has little impact on insulin-stimulated glucose uptake into the muscle or on systemic glucose disposal under insulin-stimulated conditions. These data provide evidence against a central role for the glucose/fatty cycle in regulating glucose uptake although a significant role for PDH in the reciprocal regulation of glucose and fatty acid oxidation is still evident. Additionally, we believe that therapies that increase glucose oxidation in muscle may not have a meaningful impact on glucose uptake unless paralleled by an increase in energy expenditure.

ACKNOWLEDGMENTS

We thank the staff at the Biological Testing Facility at the Garvan Institute for assistance with animal care. G. Cooney is the guarantor of this work and, as such, had full access to all the data in the study and takes responsibility for the integrity of the data and the accuracy of the data analysis. This research was facilitated by access to Sydney Mass Spectrometry, a core research facility at the University of Sydney.

GRANTS

This work was supported by the Australian Government Department of Health National Health and Medical Research Council (Grant ID 1003313, 535921). L. Small is supported by the University of New South Wales and Australian Postgraduate Awards. A portion of this work was presented at the Diabetes Keystone Symposia 2017, Keystone, Colorado, January 22–26, 2018.

DISCLOSURES

No conflicts of interest, financial or otherwise, are declared by the authors.

AUTHOR CONTRIBUTIONS

L.S. and G.J.C. conceived and designed research; L.S., A.E.B., L.E.Q, and J.R.K. performed experiments; L.S., L.E.Q. and J.R.K. analyzed data; L.S. interpreted results of experiments; L.S. prepared figures; L.S. drafted manuscript; L.S., A.E.B., D.E.J., N.T., and G.J.C. edited and revised manuscript; G.J.C. approved final version of manuscript.

REFERENCES

1. **Backshear PJ, Holloway PA, Alberti KG.** Metabolic interactions of dichloroacetate and insulin in experimental diabetic ketoacidosis. *Biochem J* 146: 447–456, 1975. doi:10.1042/bj1460447.
2. **Blackshear PJ, Holloway PA, Alberti KG.** The metabolic effects of sodium dichloroacetate in the starved rat. *Biochem J* 142: 279–286, 1974. doi:10.1042/bj1420279.
3. **Bowker-Kinley MM, Davis WI, Wu P, Harris RA, Popov KM.** Evidence for existence of tissue-specific regulation of the mammalian pyruvate dehydrogenase complex. *Biochem J* 329: 191–196, 1998. doi:10.1042/bj3290191.
4. **Brown JA, Gore DC.** In vivo metabolic response of glucose to dichloroacetate in humans. *J Surg Res* 61: 391–394, 1996. doi:10.1006/jsre.1996.0135.
5. **Cherrington AD.** Banting Lecture 1997. Control of glucose uptake and release by the liver in vivo. *Diabetes* 48: 1198–1214, 1999. doi:10.2337/diabetes.48.5.1198.
6. **Clark AS, Mitch WE, Goodman MN, Fagan JM, Goheer MA, Curnow RT.** Dichloroacetate inhibits glycolysis and augments insulin-stimulated glycogen synthesis in rat muscle. *J Clin Invest* 79: 588–594, 1987. doi:10.1172/JCI112851.
7. **Constantin-Teodosiu D, Constantin D, Stephens F, Laithwaite D, Greenhaff PL.** The role of FOXO and PPAR transcription factors in diet-mediated inhibition of PDC activation and carbohydrate oxidation during exercise in humans and the role of pharmacological activation of PDC in overriding these changes. *Diabetes* 61: 1017–1024, 2012. doi:10.2337/db11-0799.
8. **Constantin-Teodosiu D, Stephens FB, Greenhaff PL.** Perpetual muscle PDH activation in PDH kinase knockout mice protects against high-fat feeding-induced muscle insulin resistance. *Proc Natl Acad Sci USA* 112: E824–E824, 2015. doi:10.1073/pnas.1422929112.
9. **Coore HG, Denton RM, Martin BR, Randle PJ.** Regulation of adipose tissue pyruvate dehydrogenase by insulin and other hormones. *Biochem J* 125: 115–127, 1971. doi:10.1042/bj1250115.
10. **Engel PC, Jones JB.** Causes and elimination of erratic blanks in enzymatic metabolite assays involving the use of NAD+ in alkaline hydrazine buffers: improved conditions for the assay of L-glutamate, L-lactate, and other metabolites. *Anal Biochem* 88: 475–484, 1978. doi:10.1016/0003-2697(78)90447-5.
11. **Fox AW, Sullivan BW, Buffini JD, Neichin ML, Nicora R, Hoehler FK, O'Rourke R, Stoltz RR.** Reduction of serum lactate by sodium dichloroacetate, and human pharmacokinetic-pharmacodynamic relationships. *J Pharmacol Exp Ther* 279: 686–693, 1996.
12. **Gao J, Islam MA, Brennan CM, Dunning BE, Foley JE.** Lactate clamp: a method to measure lactate utilization in vivo. *Am J Physiol Endocrinol Metab* 275: E729–E733, 1998.
13. **Guo Z.** Pyruvate dehydrogenase, Randle cycle, and skeletal muscle insulin resistance. *Proc Natl Acad Sci USA* 112: E2854, 2015. doi:10.1073/pnas.1505398112.
14. **Holness MJ, Kraus A, Harris RA, Sugden MC.** Targeted upregulation of pyruvate dehydrogenase kinase (PDK)-4 in slow-twitch skeletal muscle underlies the stable modification of the regulatory characteristics of PDK induced by high-fat feeding. *Diabetes* 49: 775–781, 2000. doi:10.2337/diabetes.49.5.775.

15. **Howlett RA, Heigenhauser GJ, Hultman E, Hollidge-Horvat MG, Spriet LL.** Effects of dichloroacetate infusion on human skeletal muscle metabolism at the onset of exercise. *Am J Physiol Endocrinol Metab* 277: E18–E25, 1999.
16. **Hue L, Taegtmeyer H.** The Randle cycle revisited: a new head for an old hat. *Am J Physiol Endocrinol Metab* 297: E578–E591, 2009. doi:10.1152/ajpendo.00093.2009.
17. **Hwang B, Jeoung NH, Harris RA.** Pyruvate dehydrogenase kinase isoenzyme 4 (PDHK4) deficiency attenuates the long-term negative effects of a high-saturated fat diet. *Biochem J* 423: 243–252, 2009. doi:10.1042/BJ20090390.
18. **Iannello S, Campione R, Belfiore F.** Response of insulin, glucagon, lactate, and nonesterified fatty acids to glucose in visceral obesity with and without NIDDM: relationship to hypertension. *Mol Genet Metab* 63: 214–223, 1998. doi:10.1006/mgme.1997.2670.
19. **James DE, Jenkins AB, Kraegen EW.** Heterogeneity of insulin action in individual muscles in vivo: euglycemic clamp studies in rats. *Am J Physiol Endocrinol Metab* 248: E567–E574, 1985. doi:10.1152/ajpendo.1985.248.5.E567.
20. **James MO, Jahn SC, Zhong G, Smeltz MG, Hu Z, Stacpoole PW.** Therapeutic applications of dichloroacetate and the role of glutathione transferase zeta-1. *Pharmacol Ther* 170: 166–180, 2017. doi:10.1016/j.pharmthera.2016.10.018.
21. **Jeoung NH, Harris RA.** Pyruvate dehydrogenase kinase-4 deficiency lowers blood glucose and improves glucose tolerance in diet-induced obese mice. *Am J Physiol Endocrinol Metab* 295: E46–E54, 2008. doi:10.1152/ajpendo.00536.2007.
22. **Keung W, Ussher JR, Jaswal JS, Raubenheimer M, Lam VHM, Wagg CS, Lopaschuk GD.** Inhibition of carnitine palmitoyltransferase-1 activity alleviates insulin resistance in diet-induced obese mice. *Diabetes* 62: 711–720, 2013. doi:10.2337/db12-0259.
23. **Kim YI, Lee FN, Choi WS, Lee S, Youn JH.** Insulin regulation of skeletal muscle PDK4 mRNA expression is impaired in acute insulin-resistant states. *Diabetes* 55: 2311–2317, 2006. doi:10.2337/db05-1606.
24. **Kulkarni SS, Salehzadeh F, Fritz T, Zierath JR, Krook A, Osler ME.** Mitochondrial regulators of fatty acid metabolism reflect metabolic dysfunction in type 2 diabetes mellitus. *Metabolism* 61: 175–185, 2012. doi:10.1016/j.metabol.2011.06.014.
25. **Lee I-K.** The role of pyruvate dehydrogenase kinase in diabetes and obesity. *Diabetes Metab J* 38: 181–186, 2014. doi:10.4093/dmj.2014.38.3.181.
26. **Lovejoy J, Mellen B, Digirolamo M.** Lactate generation following glucose ingestion: relation to obesity, carbohydrate tolerance and insulin sensitivity. *Int J Obes* 14: 843–855, 1990.
27. **Lovejoy J, Newby FD, Gebhart SS, DiGirolamo M.** Insulin resistance in obesity is associated with elevated basal lactate levels and diminished lactate appearance following intravenous glucose and insulin. *Metabolism* 41: 22–27, 1992. doi:10.1016/0026-0495(92)90185-D.
28. **Nellemann B, Vendelbo MH, Nielsen TS, Bak AM, Høgild M, Pedersen SB, Biensø RS, Pilegaard H, Møller N, Jessen N, Jørgensen JOL.** Growth hormone-induced insulin resistance in human subjects involves reduced pyruvate dehydrogenase activity. *Acta Physiol (Oxf)* 210: 392–402, 2014. doi:10.1111/apha.12183.
29. **Nuutila P, Peltoniemi P, Oikonen V, Larmola K, Kemppainen J, Takala T, Sipilä H, Oksanen A, Ruotsalainen U, Bolli GB, Yki-Järvinen H.** Enhanced stimulation of glucose uptake by insulin increases exercise-stimulated glucose uptake in skeletal muscle in humans: studies using [15O]O2, [15O]H2O, [18F]fluoro-deoxy-glucose, and positron emission tomography. *Diabetes* 49: 1084–1091, 2000. doi:10.2337/diabetes.49.7.1084.
30. **Oakes ND, Bell KS, Furler SM, Camilleri S, Saha AK, Ruderman NB, Chisholm DJ, Kraegen EW.** Diet-induced muscle insulin resistance in rats is ameliorated by acute dietary lipid withdrawal or a single bout of exercise: parallel relationship between insulin stimulation of glucose uptake and suppression of long-chain fatty acyl-CoA. *Diabetes* 46: 2022–2028, 1997. doi:10.2337/diab.46.12.2022.
31. **Oakes ND, Cooney GJ, Camilleri S, Chisholm DJ, Kraegen EW.** Mechanisms of liver and muscle insulin resistance induced by chronic high-fat feeding. *Diabetes* 46: 1768–1774, 1997. doi:10.2337/diab.46.11.1768.
32. **Patel MS, Nemeria NS, Furey W, Jordan F.** The pyruvate dehydrogenase complexes: structure-based function and regulation. *J Biol Chem* 289: 16615–16623, 2014. doi:10.1074/jbc.R114.563148.
33. **Petersen MC, Rahimi Y, Camporez J-PG, Pesta D, Perry RJ, Jurczak MJ, Cline GW, Shulman GI.** Reply to Constantin-Teodosiu et al.: mice with genetic PDH activation are not protected from high-fat diet-induced muscle insulin resistance. *Proc Natl Acad Sci USA* 112: E825–E825, 2015. doi:10.1073/pnas.1423574112.
34. **Qvisth V, Hagström-Toft E, Moberg E, Sjöberg S, Bolinder J.** Lactate release from adipose tissue and skeletal muscle in vivo: defective insulin regulation in insulin-resistant obese women. *Am J Physiol Endocrinol Metab* 292: E709–E714, 2007. doi:10.1152/ajpendo.00104.2006.
35. **Rahimi Y, Camporez J-PG, Petersen MC, Pesta D, Perry RJ, Jurczak MJ, Cline GW, Shulman GI.** Genetic activation of pyruvate dehydrogenase alters oxidative substrate selection to induce skeletal muscle insulin resistance. *Proc Natl Acad Sci USA* 111: 16508–16513, 2014. doi:10.1073/pnas.1419104111.
36. **Randle PJ, Garland PB, Hales CN, Newsholme EA.** The glucose fatty-acid cycle. Its role in insulin sensitivity and the metabolic disturbances of diabetes mellitus. *Lancet* 1: 785–789, 1963. doi:10.1016/S0140-6736(63)91500-9.
37. **Reznick J, Preston E, Wilks DL, Beale SM, Turner N, Cooney GJ.** Altered feeding differentially regulates circadian rhythms and energy metabolism in liver and muscle of rats. *Biochim Biophys Acta* 1832: 228–238, 2013. doi:10.1016/j.bbadis.2012.08.010.
38. **Rinnankoski-Tuikka R, Silvennoinen M, Torvinen S, Hulmi JJ, Lehti M, Kivelä R, Reunanen H, Kainulainen H.** Effects of high-fat diet and physical activity on pyruvate dehydrogenase kinase-4 in mouse skeletal muscle. *Nutr Metab (Lond)* 9: 53, 2012. doi:10.1186/1743-7075-9-53.
39. **Saghir SA, Schultz IR.** Low-dose pharmacokinetics and oral bioavailability of dichloroacetate in naive and GST-zeta-depleted rats. *Environ Health Perspect* 110: 757–763, 2002. doi:10.1289/ehp.02110757.
40. **Shulman GI, Rothman DL, Jue T, Stein P, DeFronzo RA, Shulman RG.** Quantitation of muscle glycogen synthesis in normal subjects and subjects with non-insulin-dependent diabetes by 13C nuclear magnetic resonance spectroscopy. *N Engl J Med* 322: 223–228, 1990. doi:10.1056/NEJM199001253220403.
41. **Stacpoole PW, Greene YJ.** Dichloroacetate. *Diabetes Care* 15: 785–791, 1992. doi:10.2337/diacare.15.6.785.
42. **Stacpoole PW, Henderson GN, Yan Z, James MO.** Clinical pharmacology and toxicology of dichloroacetate. *Environ Health Perspect* 106, *Suppl* 4: 989–994, 1998. doi:10.1289/ehp.98106s4989.
43. **Stacpoole PW, Moore GW, Kornhauser DM.** Metabolic effects of dichloroacetate in patients with diabetes mellitus and hyperlipoproteinemia. *N Engl J Med* 298: 526–530, 1978. doi:10.1056/NEJM197803092981002.
44. **Tao R, Xiong X, Harris RA, White MF, Dong XC.** Genetic inactivation of pyruvate dehydrogenase kinases improves hepatic insulin resistance induced diabetes. *PLoS One* 8: e71997, 2013. doi:10.1371/journal.pone.0071997.
45. **Turner N, Bruce CR, Beale SM, Hoehn KL, So T, Rolph MS, Cooney GJ.** Excess lipid availability increases mitochondrial fatty acid oxidative capacity in muscle: evidence against a role for reduced fatty acid oxidation in lipid-induced insulin resistance in rodents. *Diabetes* 56: 2085–2092, 2007. doi:10.2337/db07-0093.
46. **Turner N, Kowalski GM, Leslie SJ, Risis S, Yang C, Lee-Young RS, Babb JR, Meikle PJ, Lancaster GI, Henstridge DC, White PJ, Kraegen EW, Marette A, Cooney GJ, Febbraio MA, Bruce CR.** Distinct patterns of tissue-specific lipid accumulation during the induction of insulin resistance in mice by high-fat feeding. *Diabetologia* 56: 1638–1648, 2013. doi:10.1007/s00125-013-2913-1.
47. **Wright LE, Brandon AE, Hoy AJ, Forsberg G-B, Lelliott CJ, Reznick J, Löfgren L, Oscarsson J, Strömstedt M, Cooney GJ, Turner N.** Amelioration of lipid-induced insulin resistance in rat skeletal muscle by overexpression of Pgc-1β involves reductions in long-chain acyl-CoA levels and oxidative stress. *Diabetologia* 54: 1417–1426, 2011. doi:10.1007/s00125-011-2068-x.
48. **Wu P, Sato J, Zhao Y, Jaskiewicz J, Popov KM, Harris RA.** Starvation and diabetes increase the amount of pyruvate dehydrogenase kinase isoenzyme 4 in rat heart. *Biochem J* 329: 197–201, 1998. doi:10.1042/bj3290197.
49. **Yuan M, Breitkopf SB, Yang X, Asara JM.** A positive/negative ion-switching, targeted mass spectrometry-based metabolomics platform for bodily fluids, cells, and fresh and fixed tissue. *Nat Protoc* 7: 872–881, 2012. doi:10.1038/nprot.2012.024.